Journal of Medical Entomology, 57(2), 2020, 353–368
doi: 10.1093/jme/tjz188
Advance Access Publication Date: 1 November 2019
Research

Waveforms From Stylet Probing of the Mosquito *Aedes aegypti* (Diptera: Culicidae) Measured by AC–DC Electropenetrography

Astri C. Wayadande,[1,4] Elaine A. Backus,[2] Bruce H. Noden,[1,©] and Timothy Ebert[3]

[1]Department of Entomology and Plant Pathology, 127 Noble Research Center, Oklahoma State University, Stillwater, OK 74078, [2]USDA-Agricultural Research Service, San Joaquin Valley Agricultural Sciences Center, 9611 South Riverbend Avenue, Parlier, CA 93648, [3]University of Florida, Citrus Research and Education Center, 700 Experiment Station Drive, Lake Alfred, FL 33850, and [4]Corresponding author, e-mail: a.wayadande@okstate.edu

Subject Editor: Julian Hillyer

Received 13 June 2019; Editorial decision 28 September 2019

Abstract

Electropenetrography (EPG) has been used for many years to visualize unseen stylet probing behaviors of plant-feeding piercing–sucking insects, primarily hemipterans. Yet, EPG has not been extensively used with blood-feeding insects. In this study, an AC–DC electropenetrograph with variable input resistors (Ri), i.e., amplifier sensitivities, was used to construct a waveform library for the mosquito arbovirus vector, *Aedes aegypti* (Linneaus), while feeding on human hands. EPG waveforms representing feeding activities were: 1) electrically characterized, 2) defined by visual observation of biological activities, 3) analyzed for differences in appearance by Ri level and type of applied signal (AC or DC), and 4) quantified. Electrical origins of waveforms were identified from five different Ri levels and AC versus DC. Mosquitoes produced short stylet probes ('bites') that typically contained five waveform families. Behaviors occurred in the following order: surface salivation (waveform family J), stylet penetration through the outer skin (K), penetration of deeper tissues and location of blood vessels/pathway activities (L), active ingestion with engorgement (M), and an unknown behavior that terminated the probe (N). Only K, L, and M were performed by every insect. A kinetogram of conditional probabilities for waveform performance demonstrated plasticity among individuals in L and M, which were alternated. Now that EPG waveforms for mosquito feeding have been defined, EPG can be used as a tool for improved biological understanding of mosquito-borne diseases.

Key Words: vector, arbovirus, pathogen transmission, waveform library, electropenetrography

Vector-borne diseases are responsible for about 20% of all infectious human diseases worldwide, causing almost a million deaths annually. While some, such as malaria and dengue, have stably impacted populations for centuries, others (e.g., yellow fever) have re-emerged, or have invaded new regions of the world (e.g., chikungunya and zika viruses) (WHO 2017). Very little is known about the stylet probing behaviors of human-infecting mosquito vectors. The increase of vector-borne diseases highlights the need for better understanding of mosquito feeding, to aid in developing new and novel targets in the disease cycle.

One new research area of the last 20 years has focused on mosquito–host interactions occurring through the attraction and feeding process. Beginning at the host detection phase, mosquitoes use CO_2, odorants, heat, and visual cues to find landing places on hosts (Zhou et al. 2018). Much attention has been given to the role of odor in the host detection and feeding process and the impact of various olfactory receptors, from structural to genetic levels (Zwiebel and Takken 2004, Ray 2015, Lutz et al. 2017). Host-seeking behavior in mosquitoes is mediated by receptors on the antennae, palps, and proboscis (Maekawa et al. 2011). Recently, mosquito host-seeking has been reported to be affected by skin microbiota and altered emissions that occur due to *Plasmodium* infection (Robinson et al. 2018).

Other studies have focused on the mechanics of the feeding process. In 2012, stylet probing behavior of anophelines was video-recorded inside a mouse ear (Choumet et al. 2012). Gurera et al. (2018) reviewed and demonstrated how the engineering of the mosquito proboscis apparatus could be directly used in biomedical science. Recent initiatives are even developing direct feeding assays to validate their anti-malarial vaccines (Brickley et al. 2016). However, these initiatives assume that mosquito blood-feeding processes are always the same within or among species and do not vary between different hosts or sexes. In other piercing–sucking insects

(e.g., phytophagous hemipterans like aphids, leafhoppers, whiteflies, etc.), it has long been established that plasticity in feeding behavior exists within or among species in a genus, or with feeding on different host plants of a single species. Does such plasticity exist among different mosquito species on the same host? Perhaps probing by the same mosquito could vary on different human or alternate hosts. The latter seems likely, because the insightful video study of Choumet et al. (2012) demonstrated two methods of feeding, direct blood vessel puncture and pool feeding. Thus, mosquitoes can probably alter their probing methods based on environmental cues or other circumstances. If so, is such plasticity epidemiologically important? To answer these questions and many others, there is a need to develop an assay that can observe feeding internal to the host in real time, so that researchers can precisely identify, quantify, and statistically compare how multiple mosquitoes differ in their feeding processes. With such a tool, researchers will be able to study a wide range of topics regarding how mosquitoes interact with their hosts during feeding. This paper introduces just such a tool to the mosquito research community.

Electropenetrography (EPG) is a technique that allows researchers to observe, record, and quantify the feeding behaviors of arthropods whose mouthparts penetrate opaque host tissues, and therefore cannot be easily visualized in real time. This revolutionary technology was originally invented 55 y ago (McLean and Kinsey 1964) to study feeding behaviors of herbivorous insects on plants. A few years later, Kashin and colleagues (Kashin and Wakeley 1965, Kashin 1966, Kashin and Arneson 1969) developed a similar device to make the first recordings of mosquito feeding, calling their instrument the 'bitometer'. These were the only papers published using this method with mosquitoes, and in the intervening years, the revolution in electronics has enabled instruments, computers, and EPG researchers to move far beyond the important advances made in the 1960s.

In the last 50 years, EPG has been widely used in studies of feeding behavior/physiology of plant-feeding, piercing–sucking hemipteroid insects such as thrips, aphids, psyllids, leafhoppers, planthoppers, and true bugs, resulting in ~600 publications to date. EPG has been critical for gaining insights into and improvements in pest management, such as: 1) targeting insecticide modes of action (Serikawa et al. 2012, Tariq et al. 2017), 2) improving host plant resistance (Jing et al. 2015, Rangasamy et al. 2015), understanding pathogen acquisition and inoculation (Wayadande and Nault 1994), and 3) tracing targets for RNAi (Mutti et al. 2008). The underlying science and applications of EPG was recently reviewed by Backus et al. (2019).

EPG instruments have undergone three major generations of design (AC EPG by McLean and Kinsey 1964, DC EPG by Tjallingii 1978, and AC–DC EPG by Backus and Bennett 2009), but the basic principle remains the same. An AC (alternating current) or DC (direct current) signal is conveyed to the food/host (hereafter termed substrate) via a referent electrode in the soil (Backus et al. 2019). The arthropod (tethered with a recording electrode of thin, solid-gold wire glued to its cuticle) is placed on the substrate. When it inserts its mouthparts, current is conveyed through the arthropod to the instrument (Walker 2000, Backus et al. 2019) for signal processing and then to a computer for display and further analysis. Variations of voltage over time create electrical patterns (waveforms) displayed on the computer. These waveforms are correlated with highly specific behaviors, such as stylet movements and direction of fluid flow (Joost et al. 2006, Dugravot et al. 2008), salivation and ingestion (McLean and Kinsey 1967), puncturing of specific cells (Tjallingii and Hogen Esch 1993), and pathogen acquisition/inoculation (Fereres and Collar 2001, Tjallingii and Prado 2001). Other studies have been cited in reviews (Walker 2000, Backus et al. 2019).

Type of signal applied to a substrate (AC versus DC) has recently been shown to affect feeding behavior of arthropods usually larger than mosquitoes (e.g., phytophagous heteropterans) (Backus 2016, Backus et al. 2019). Any voltage level of DC can decrease amount of feeding or (at high voltages) cause complete cessation of feeding; in contrast, only high voltages of AC can cause slight irritability but no decrease in feeding (Backus 2016; E. A. Backus, unpublished data). Therefore, choice of applied voltage type is important in applications of EPG to new types of arthropods.

Waveforms are derived from electrical currents carried by electrolyte-laden fluids in the insect's stylet canals and anterior foregut. In EPG science, the instrument detects a mixture of two 'electrical origins': the R and emf components of the signal (Tjallingii 1985, Backus et al. 2019). The R component is caused by conductance of or resistance to the applied electrical signal from the instrument, i.e., fluids of different levels of conductivity (saliva, plant sap, blood) flowing through stylet canals that can impose various types of resistance (i.e., narrow or wide canal diameter, open or closed valves in the foregut). The electromotive force (emf) component is caused by biopotentials (literally, biological voltages) generated by the behaviors of the insect interacting with the electrical environment of the host, independent of the applied signal from the instrument. For example, biopotentials can be caused by insect stylets breaking cell membranes in the host or streaming of ionized fluids moving rapidly through narrow mouthpart channels. Accordingly, each EPG waveform is composed of a unique blend of R and emf, based on the underlying biophysical mechanisms of the interaction between insect and host anatomy and physiology.

An important tool to understand the contribution of R and emf to waveform structure is the waveform library. A waveform library is a collection of waveform images at different Ri levels with their accompanying interpretation of electrical origins, allowing a researcher to deduce underlying biological meanings. This value of waveform libraries for interpreting waveforms will be particularly important for studies of mosquitoes and other blood-feeding arthropods. EPG waveforms representing plant-feeding hemipteran behavior are often defined using histological correlations of sectioned plant tissue probed by recorded insects. However, especially in studies of mosquito feeding on human hosts, sectioning the probed tissue is not possible.

Certain EPG waveforms are dominated by R, others by emf, but most often they are a mixture. The most detailed and informative recordings capture both R and emf. The proportion of R to emf is dependent on the input resistor (Ri) (or inherent sensitivity of the first-stage amplifier) in the EPG instrument, as it interacts with the inherent resistance of the arthropod (Ra). Low to moderate Ri levels (10^6–10^7 Ohms) can detect mostly R components, high Ri levels (10^9–10^{10} Ohms) detect a mixture but mostly emf components, while the highest Ri (10^{12}–10^{13} Ohms) record exclusively emf (Tjallingii 1985, Backus et al. 2019). The ideal emf/R mixture is achieved when Ri matches the inherent resistance (Ra) of the arthropod recorded (Backus et al. 2000, 2019).

The objectives of this study were to use the AC–DC electropenetrograph to: 1) identify, name, and characterize the EPG waveforms of a globally important mosquito species, *Aedes aegypti* (Linneaus), recorded live while feeding on a human host; 2) visually correlate human sensations, mosquito body part movements, and blood engorgement with EPG waveforms; 3) create a waveform library at four Ri levels (10^6 through 10^9 Ohms) to identify electrical origins (R versus emf) of the waveforms and interpret

their underlying biological meanings; 4) compare effects of AC versus DC applied signals on the above criteria; and 5) using all of the above information, determine the best Ri settings for future EPG research on mosquitoes. Our study found five major waveform families and identified those representing proposed behaviors such as skin-surface salivation, salivation along the pathway to a blood source, ingestion of blood, salivation in a blood vessel, and termination of feeding. We also discuss many future applications for the research methods and information we have herein pioneered.

Materials and Methods

Insect Colony Maintenance

Adult female *Ae. aegypti* (Liverpool strain) were used in all recordings. Eggs stored at 2–4°C were rehydrated in tap water until larval emergence. Larvae were reared in 400 ml tap water in large plastic containers (Rubbermaid, Atlanta, GA) housed within a growth chamber at 27°C, 90% RH and 12:12 L:D photoperiod. Developing larvae were fed ground Tetramin fish food flakes (Tetra US, Blacksburg, VA) every other day. Pupae were removed to an emergence cage and held until use. Sugar water (10% [w:v] sucrose) was provided ad libitum on cotton balls. Females used were naive, i.e., they had not taken their first bloodmeal; thus, our recordings were of the insect's first bloodmeal.

Preparation of Mosquitoes for EPG

Adult females, 4–10 d post-eclosion, were chilled for 30–60 s on ice to immobilize them. Individuals were held by gentle manual suction of the abdomen using an aspirator fashioned from a glass pipette fired to fit the abdominal diameter (Fig. 1a). While the mosquito was immobilized, a small quantity of silver glue (1:1:1 [v:v:w] white glue [Elmer's Glue, Elmer's, Columbus, OH], tap water, and silver flake [Alfa Aesar, Ward Hill, MA]; recipe from Cervantes and Backus 2018) was painted onto the pronotum with a #2 insect pin and allowed to dry (Fig. 1b). A 3 cm length of 0.001 in (25.4 um) diam. gold wire (Sigmund Cohn, Mt. Vernon, NY) was attached to the painted area of the pronotum with additional silver glue (Fig. 1c). The other end of the gold wire had been previously glued to a stub (i.e., a copper wire that had previously been soldered to an escutcheon pin [brass nail]). Properly tethered mosquitoes were able to fly and walk. Tethered mosquitoes were given a 2- to 10-min acclimation period while dangling from the wire before beginning of a recording session. Each insect was recorded only once.

Human Hosts

Three adult human volunteers, two females and one male, were used as feeding hosts during mosquito EPG recordings. Each person was over 35 yr of age and self-reported to be susceptible to mosquito bites. All mosquitoes recorded for this study fed on the right hand/wrist of the human host. Most of the recordings were obtained from the knuckles or other areas on the back of the hand, but a few mosquitoes probed on the thumb or underside of the wrist. Over 85% of the mosquito recordings in this study were obtained using one of the female hosts, and therefore the data could not be analyzed for host sex differences.

Electropenetrography

A four-channel AC–DC electropenetrograph (built by Andrew Dowell, EPG Technologies, Inc., Gainesville, FL, andygator3@gmail.com) was used to record mosquito stylet probing. Different applied voltages were used for different Ri levels as follows: 10^6 and 10^7 Ohms: 150 mV; 10^8 and 10^9 Ohms: 75 mV; 10^{10} Ohms: 10 mV; 10^{13} Ohms: 0 mV. Higher voltages were used for lower Ri levels, in order to best detect R components. Voltage was applied to the host via a copper wire (substrate electrode) gripped in the left hand of the human host; the same hand that was offered to the wired insect. None of the human hosts reported being able to feel the signal voltage, AC or DC. The brass nail of a tethered mosquito was inserted into a head stage amplifier, which had six Ri settings available: 10^6, 10^7, 10^8, 10^9, 10^{10}, and 10^{13} Ohms, of which the first four (10^6–10^9 Ohms) were primarily used for this study; 10^{10} and 10^{13} Ohms were used on occasion, for brief switches during waveform L and M (see below). Otherwise, Ri level was set before mosquitoes initiated probing.

Data were collected using a DI-720 analog-to-digital converter with Windaq Pro+ acquisition software (both from DATAQ Instruments, Inc., Allentown, PA) on a Dell Inspiron laptop computer. Mosquitoes were recorded one at a time, on a single human hand. Multiple mosquitoes (1–20 individuals) were recorded on 18 different days. Mosquitoes were allowed access to human hands until performance of at least one probe (defined as beginning with stylet insertion into the skin and ending with withdrawal of the stylets from the skin) up to a maximum of six probes. The mosquito was removed and euthanized after either six sequential probes in which none consummated in ingestion (i.e., six unsuccessful probes), or after a probe that culminated in ingestion, engorgement, and

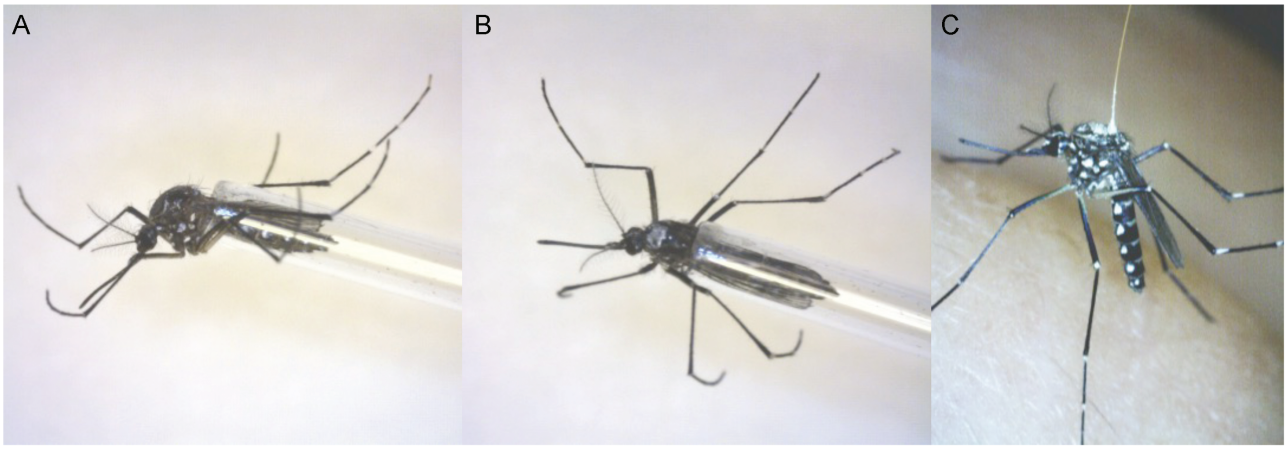

Fig. 1. Gold wire attachment to the mosquito pronotum. (A) Position of the mosquito within the fired glass pipette showing wings held back and immobilized. (B) Same mosquito with a small spot of silver glue painted onto the pronotum. (C) Same mosquito with the tether glued to the spot of silver glue on the pronotum.

repletion (i.e., a successful probe). EPG Windaq files for each mosquito were viewed and measured using Windaq Waveform Browser display software (DATAQ). Mosquito waveforms were named according to the Backus convention for hemipteran EPG waveforms, which uses a hierarchical framework with phases, families, and types (Cervantes and Backus 2018, Backus et al. 2019). Windaq gains were standardized for each Ri level (see Figs. 6 and 8). Such gains occurred after voltage acquisition, so they only impacted the size of the waveform as visualized on the computer screen (from which figures were derived) not the saved data.

Measurement and Statistical Analysis of Waveforms

Seventy-three, female, sucrose-fed (no blood) mosquitoes were wired and offered a host human hand to probe, within a Faraday cage for noise reduction. Sixty-one of those 73 females probed on a hand. Thirty-eight of those 61 females produced successful probes that reached repletion and had clear, assignable waveforms that were used for the waveform library; 41 probes from these 38 insects were incorporated into the analysis dataset. The decision to include probes from a particular female was made based upon an a priori set of criteria for inclusion in the dataset, as follows. Mosquitoes had to: 1) fly, 2) not become detached from tether, 3) probe within 10 min, and 4) produce at least one probe that was completed to repletion. Recordings were distributed among the following Ri levels: 12 for 10^6 Ohms, 12 for 10^7 Ohms, 7 for 10^8 Ohms, and 10 for 10^9 Ohms. About half of the mosquitoes were recorded using AC applied signals and the other half using DC. Fifteen additional mosquitoes were recorded, but selected waveforms were artificially terminated for correlations.

Numbers and durations of probes and behavioral (waveform) events within them varied for many mosquitoes, especially before achieving engorgement. However, we were not interested in comparing among insects for all behaviors (successful and unsuccessful probes) performed; that objective is for future studies. Instead, we were most interested in differences for each Ri level among those probes that successfully consummated in engorgement. Consequently, in most cases, we chose one probe that achieved engorgement per mosquito for measurement and analysis, although four mosquitoes each provided two probes to the dataset. The data consisted of a temporally ordered sequence of waveform events (uninterrupted occurrences of one waveform).

Waveform data were used to calculate probabilities for all transitions among waveform events for a kinetogram, plus means and SEs for six variables for each waveform, as follows: 1) number of waveform events per insect (NWEI), 2) (mean) waveform duration per insect (WDI), 3) (mean) waveform duration per event per insect (WDEI), 4) maximum waveform event duration per insect, 5) percentage of the probe represented by each waveform, per insect, and 6) time to the first event of a waveform, per insect.

To generate the above descriptive statistics and perform analyses of variance (ANOVA) on the above variables, we used a generic version of the Ebert EPG analysis program (Ebert et al. 2015), available at the EPG Workshop website: https://crec.ifas.ufl.edu/extension/epg/sas.shtml (accessed 16 March 2019). A dummy behavior for non-probing was added to the start and end of each probe with a duration of 1 s. ANOVAs were performed using Proc Glimmix, with assumptions of the model tested graphically using plots of observed versus predicted to assess heteroscedasticity, and a q-q plot to assess normality. Multiple comparisons were performed by protected Least Significant Difference (LSD) test for treatment differences between the four Ri levels: 10^6, 10^7, 10^8, and 10^9 Ohms. We used SAS version 9.4TS1M3, under Enterprise Guide 7.1.

Correlation of Waveforms With Body Movements and Stylet Activities

A 5× hand-held magnifying lens was positioned so that the human host could observe mosquito body position, stylet position, labial angle, and maxillary palp movements, for visual correlation with EPG waveforms. Blood uptake and engorgement was easily observed through the transparent cuticle of the mosquito abdomen and therefore used as a marker for ingestion. Observations of mosquito behavior and hand sensations were verbalized by the human host during mosquito probing. Audio was recorded via the iPhone Voice Memo app (Apple Inc., Cupertino, CA). Time signatures on the Windaq recording and Voice Memo app were manually synchronized in handwritten notes about the observations. Additionally, for waveforms that were recorded early in the feeding process, 15 mosquitoes were interrupted during production of the target waveform, removed from the wire, and immediately dissected and examined via a Wild M5 stereomicroscope (Wild Heerbrugg, Heerbrugg, Switzerland) for the presence of red blood cells in the gut.

Generation of *Ae. aegypti* Waveform Library

Mosquitoes were recorded at four input resistor (Ri) levels (10^6, 10^7, 10^8, and 10^9) to identify electrical origins in the resulting EPG waveforms. In addition, Ri levels of selected insects were switched to 10^{10} or 10^{13} Ohms during L and/or M waveforms (see below), to compare R and emf components while controlling for differences in individual insect behaviors and wiring quality. Comparisons of waveforms between AC and DC applied signals and for the different Ri levels were made using similar Windaq gain settings, although sometimes very tiny waveforms at high Ri levels were magnified with larger gains (see Figs. 6 and 8).

Results

Overview of *Ae. aegypti* Waveforms and Probing Activities

Adult female *Ae. aegypti* mosquitoes produced stereotypical waveforms with each probe that resulted in a bloodmeal. By definition, a probe is initiated when the tips of the stylets (fascicle) are inserted into the substrate (i.e., skin) and is completed with the withdrawal of the stylets. Upon landing on the human host, tethered mosquitoes explored the skin surface with the labial tip, rapidly tapping the surface. Insertion of the stylets was frequently observed to occur in crevices of the skin. Interestingly, pain was rarely associated with stylet insertion; however, deeper penetration was occasionally accompanied by discomfort. This was particularly evident in longer probes that took place on the underside of the human host's wrist. Discomfort was described as an intense ache, rather than a sharp pain. Stylet insertion was accompanied by bending of the labium, the angle of which became more acute with deeper insertion.

EPG revealed three clear phases (*pre-probing*, *pathway*, and *ingestion*) composed of five distinct waveform families and types within them that were given the following designations: families J, K, L (with types L1 and L2), and M (with types M1 and M2). In addition, there was one waveform family (N) of unknown meaning. Electrical characterization of the waveforms and other information from the Results are summarized in Table 1.

Several individual mosquitoes made short test probes, but usually continued until achieving engorgement in a longer probe. Unlike most hemipteran probes, which can last for several hours, 95% of *Ae. aegypti* probes were between 2 and 4 min while the longest

Table 1. Summary of categorization, electrical characterizations, and proposed biological meanings of all waveforms for *Aedes aegypti* feeding on human hand, as described in-depth in the narrative

Waveform categories and names		Waveform characterizations				Proposed biological meanings	
Phase and family	Type	Repetition rate	Best seen at these Ri levels	Description	Electrical origin	Stylet tip location	Stylet and foregut activities
Pre-probing							
J		N/A	10^8, 10^9 Ohms	Irregular	emf-dominated, some R	Skin surface	Dilute salivation on skin surface
Pathway							
K		8–12/s	10^6, 10^7 Ohms	Regular	Mixed R + emf	Outer skin layer	Shallow penetration of skin; more viscous saliva
L	L1	8–11/s	10^6, 10^7 Ohms	Regular	Mixed R + emf	Deeper in skin	Salivation and searching for a blood source
	L2	8–10/s	10^7, 10^8 Ohms	Irregular	R-dominated, some emf	Deeper in skin	Salivation and searching for a blood source
Ingestion							
M	M1	5–16/s	10^7, 10^8 Ohms	Regular	Mixed R + emf	Blood vessel	Blood ingestion in blood vessel
	M2	5–12/s	10^7, 10^8 Ohms	Irregular	R-dominated, some emf	Blood vessel	Salivation into blood vessel
Unknown							
N		N/A	All Ri levels	Irregular	R-dominated, some emf	Unknown	Unknown

probe recorded was 16 min in duration. During this short contact interval with the human host, mosquitoes rapidly reached repletion.

Appearances of AC versus DC Waveforms

Within each Ri level, most waveforms produced with AC applied voltage were nearly identical to those produced with DC voltage. Consequently, we alternated AC and DC waveforms for the main waveform library figures (Figs. 2–5). Exceptions to this similarity finding for certain waveforms will be discussed in the context of those waveforms.

Waveform Library: Phases, Families, and Types

Pre-probing Phase: Family J

Pre-probing phase was identified by preparatory movements of the stylets at the same time as performance of waveform J. The mosquito proboscis moved into a perpendicular position prior to the onset of J, which commenced once the proboscis contacted the skin. Waveform J ended when the stylets punctured the skin. Waveform J was present at all Ri levels, but it was barely visible at 10^6 and 10^7 Ohms. Especially at 10^6 Ohms, J only could be recognized by a tiny voltage peak at its outset; the rest was not or barely discernable (Figs. 2a and b and 3a and b, respectively). This inability to detect J at 10^6 Ohms resulted in only 2/12 probes having J (Table 2) and the number of waveform J events per insect being significantly lower than for any other Ri level ($F = 15.62$; df = 3, 37) (Table 2). Per event duration of J was significantly longer (waveform duration per event; WDEI) ($F = 3.19$; df = 3, 24) at 10^6 Ohms and of intermediate duration at 10^7 Ohms, compared with 10^8 and 10^9 Ohms, which were not significantly different from each other (Table 2). Similarly, while J represented only a small percentage of the total probing duration for each Ri level, this percentage was significantly ($F = 5.55$; df = 3, 37) lowest for 10^6 Ohms, intermediate for 10^7 Ohms, and highest for 10^8 and 10^9 Ohms, which were not significantly different (Table 2).

Above Ri 10^7 Ohms, tiny voltage fluctuations began to appear during J (Fig. 4a and b for 10^8 Ohms), forming more distinct patterns more easily discernable as waveforms. At Ri 10^9 Ohms, J started with a very short spike (lasting 0.1–0.2 s) (Fig. 5a, asterisk) followed by a wave that gradually rose in amplitude and formed a voltage hump that terminated just as the stylets penetrated the skin (Fig. 5a, inset boxes). At Ri 10^{10}, J was very apparent with a very large voltage hump before stylet penetration (Fig. 6b, arrow). Waveform J generally represented a short duration activity of 2–5 s, but longer J events were occasionally recorded (Table 2).

The above changes in waveform appearance with Ri level indicate that most of J was a heavily emf-dominated waveform. We concluded this because J was not seen at most Ri levels, despite clearly visible performance of the same overt mosquito behavior (stylet contact on host skin while stylets were held at a right angle) at all Ri levels. Only at Ri 10^9 Ohms or higher was any signal visible, and that was only a small voltage level-shift or hump. That said, the tiny voltage peak at the start of the probe was due to a mixed R-emf (but mostly R) component, visible at all Ri levels. Thus, while J was emf, there was also a small amount of R.

Pathway Phase: Family K

Presumed stylet insertion into the skin began the earliest part of the recording, pathway phase. The first waveform family of pathway phase was family K. It was impossible to directly observe insertion of the stylet tips because they were ensheathed by the labium; however, insertion was inferred from proboscis position being perpendicular to the skin surface, rapid lateral movements back-and-forth of the proximal end of the proboscis and alternating up-and-down labial palpus movements that coincided with rapid peak oscillations and high deflection from the baseline. At low Ri levels (10^6 and 10^7) each probe started with a frequency of 8–12 Hz, as a series of short spikes that quickly rose in amplitude like a staircase followed by 3–10 larger peaks at the same frequency that rose from a higher voltage level that formed a hump 1–2 s in duration (Figs. 2a and b and 3a and b). At higher Ri levels (10^8 and 10^9 Ohms), the appearance of the spikes and peaks degenerated. At 10^9 Ohms, the spikes and peaks were barely discernable, and K was largely recognized by the voltage hump.

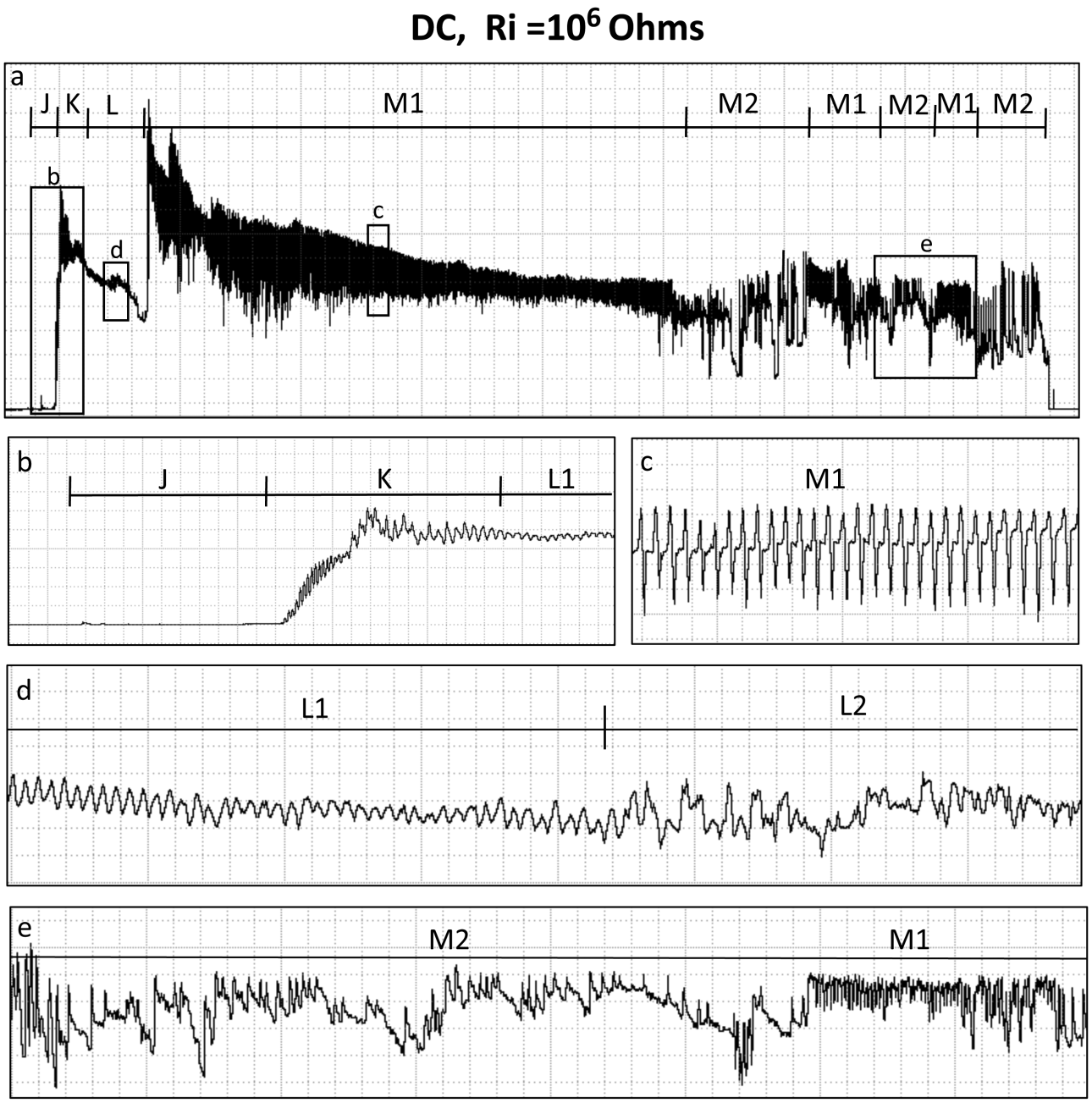

Fig. 2. Representative waveforms for EPG recordings at Ri = 10^6 Ohms, using applied signal of 150 mV DC. (a) Overview of the entire mosquito stylet probe ('bite'). Family- and type-level names are along the top of the label bar. (b–e) Enlargements of boxes b–e in part (a). Labels similar to part (a). Time scales and Windaq gains were as follows: (a) 9.2 s/div, 8×; (b) 0.8 s/div, 8×; (c) 0.2 s/div, 8×; (d) 0.2 s/div, 64×; (e) 0.2 s/div, 8×.

The above differences among the appearances of K at different Ri levels were essentially the same for AC versus DC applied voltages, as demonstrated in Fig. 6. Slight differences within each Ri level were unique to individual mosquitoes. The only significant quantitative difference among the Ri levels was for WDEI. The duration of K events was longest for 10^6 Ohms, intermediate for 10^7 Ohms, and shortest for 10^8 and 10^9 Ohms, which were not significantly different (Table 2).

Thus, as with J, Ri level was critical in the recognition of K. This finding supports that the spikes and peaks of K were R-dominated, while the voltage level hump was emf-dominated. Usually, there was no pain for the human host associated with waveform K. However, occasionally the human host reported feeling a skin prick during the instant of stylet insertion. Therefore, K was associated with shallow stylet insertion.

Family L

Following K, the voltage level gradually decreased to a relatively steady level with superimposed small peaklets; this waveform family was termed L. At low Ri levels (especially 10^6 Ohms), waveform L moved steadily downward (less positive) in voltage level, while at higher Ri levels, the L voltage level was mostly flat. There were no significant differences in numbers (NWEI), event durations (WDEI), or percentage of total probing represented by L (Table 2).

Family L was divided into two waveform types, L1 and L2 (Figs. 2d, 3d, and 4d). L1 was a highly regular and rhythmic pattern with a steady frequency (8–11 Hz; Table 1) of small sine-wave peaks of much smaller amplitude than that of M (see below). The rhythmic L1 fine structure rapidly degraded into L2 after 10–60 s. While L2 was at a

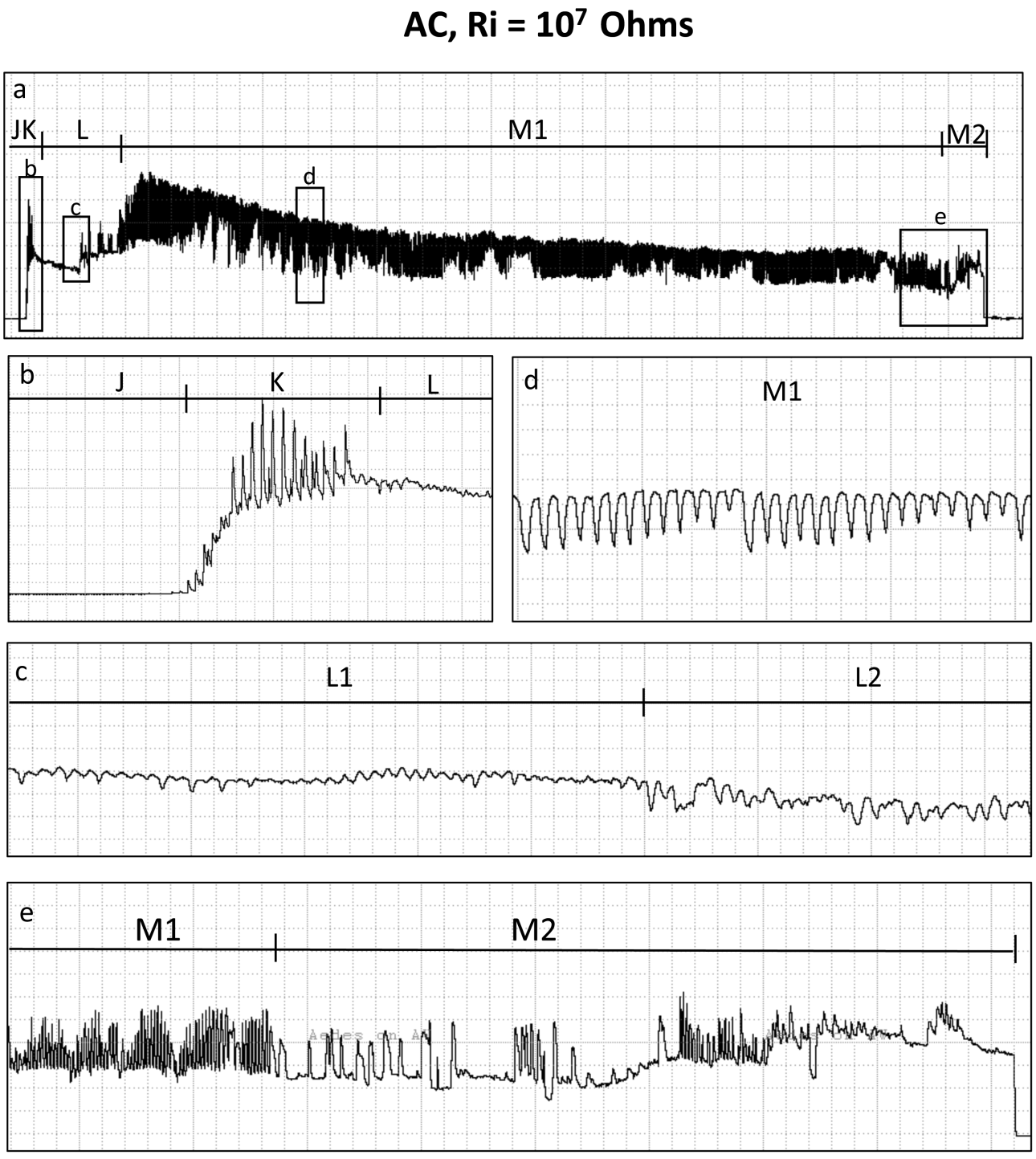

Fig. 3. Representative waveforms for EPG recordings at Ri = 10^7 Ohms, using applied signal of 150 mV AC. (a) Overview of the entire mosquito stylet probe ('bite'). Family- and type-level names are along the top of the label bar. (b–e) Enlargements of boxes b–e in part (a). Labels similar to part (a). Time scales and Windaq gains were as follows: (a) 13 s/div, 8×; (b) 0.6 s/div, 8×; (c) 0.2 s/div, 32×, inset: 64×; (d) 0.2 s/div, 8×.

similar voltage level as L1, it was different and recognizable because of its irregular amplitude with variable-frequency and -amplitude peaks and tiny spikes. These L2 spikes and peaks were distinctly visible at 10^6 Ohms (Fig. 2d). As Ri level increased, L2 spikes and peaks became smoother and smaller in amplitude (Figs. 3d and 4d). At 10^9 Ohms (for DC applied signal, 10^{10} Ohms for AC signal), L2 separated into two subtypes (not named, though one could, in future research). Most of L2 at 10^9 or 10^{10} Ohms was a smaller version of L2 at 10^8 Ohms, with even smaller, irregular peaks and spikes. However, occasionally, for a few seconds, the waveform became a nearly flat line. Thus, a tiny remnant of fluctuating L2 (emf component) remained at 10^9 or 10^{10} Ohms, while another part of L2 disappeared entirely (thus, was an R component) at the same Ri levels. Accordingly, similar to K, the fine structure and changing voltage levels of L were primarily caused by resistance (R component), while the amplitude hump and a tiny fraction of rhythmicity of L1 was caused by emf.

During L1, there was a visible and consistent correlation with flapping movements of the maxillary palpi back and forth, although

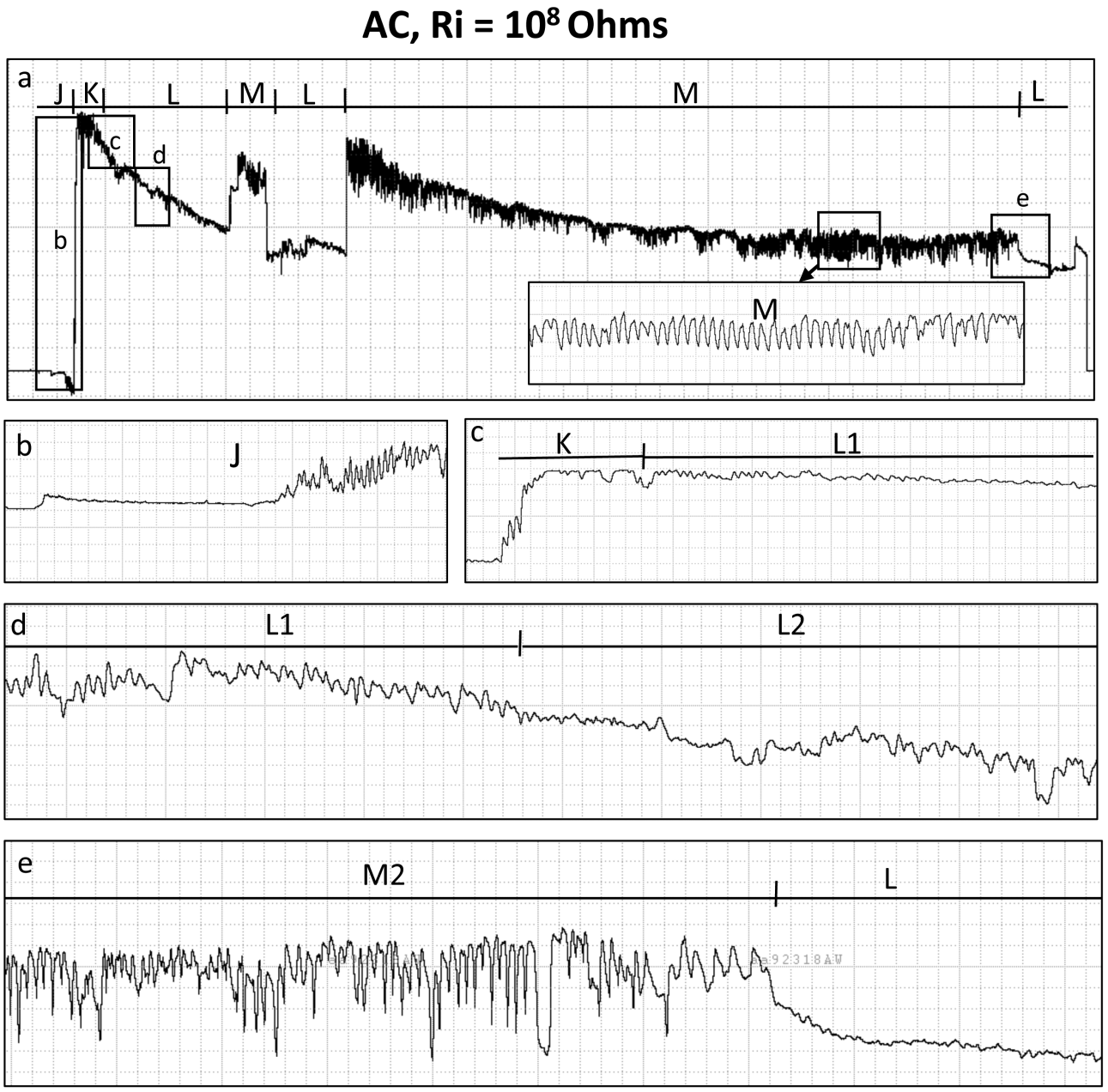

Fig. 4. Representative waveforms for EPG recordings at Ri = 10^8 Ohms, using applied signal of 75 mV AC. (a) Overview of the entire mosquito stylet probe ('bite'). Family- and type-level names are along the top of the label bar. (b–e) Enlargements of boxes b–e in part (a). Labels similar to part (a). Time scales and Windaq gains were as follows: (a) 5 s/div, 4×, inset: 0.2 s/div, 8×; (b) 0.2 s/div, 16×; (c) 0.2 s/div, 2×; (d) 0.2 s/div, 16×; (e) 0.2 s/div, 16×.

the frequency of L1 was much higher than the frequency of palpi flapping. Maxillary palpi movements were absent during L2. Also, both L subtypes were almost always correlated with gradually increased bending of the labium, thus shortening of the stylets left outside the human host. Duration of L was variable, ranging from 17 to 153 s (Table 2). Blood was only observed when the mosquito initiated the next phase, M (N = 8), even when the M duration was very short (2–3 s). Family L was also visually correlated with partial stylet withdrawal (uplift of head and straightening of the previously bent proboscis) and re-penetration.

Ingestion Phase: Family M

After pre-probing (J) and pathway (K and L) phases were completed, *Ae. aegypti* began ingesting a bloodmeal during waveform family M (Figs. 2a, c, and e; 3a and c; 4a; and 5a and c). At all Ri levels, M was identified by a sudden rise in voltage level, usually to the highest or nearly highest level in the probe (e.g., Figs. 2a, 3a, and 4a). The degree of rise in voltage level increased with increasing Ri, therefore the rise was an emf component. After the abrupt rise, when Ri levels were 10^6–10^8 Ohms, voltage level of M would gradually decline before leveling off. At the same Ri levels, amplitude of the M waveform peaks (both types, see below) would start out very high and gradually decrease to the lowest amplitude at the steady voltage level, although M amplitude also varied over time within the same probe (Figs. 2a, 3a, and 4a) and in successive probes by the same insect on the same hand (data not shown). In contrast, at Ri 10^9 Ohms, voltage level was mostly steady, and amplitude of M peaks was uniformly small; voltage level and amplitude were

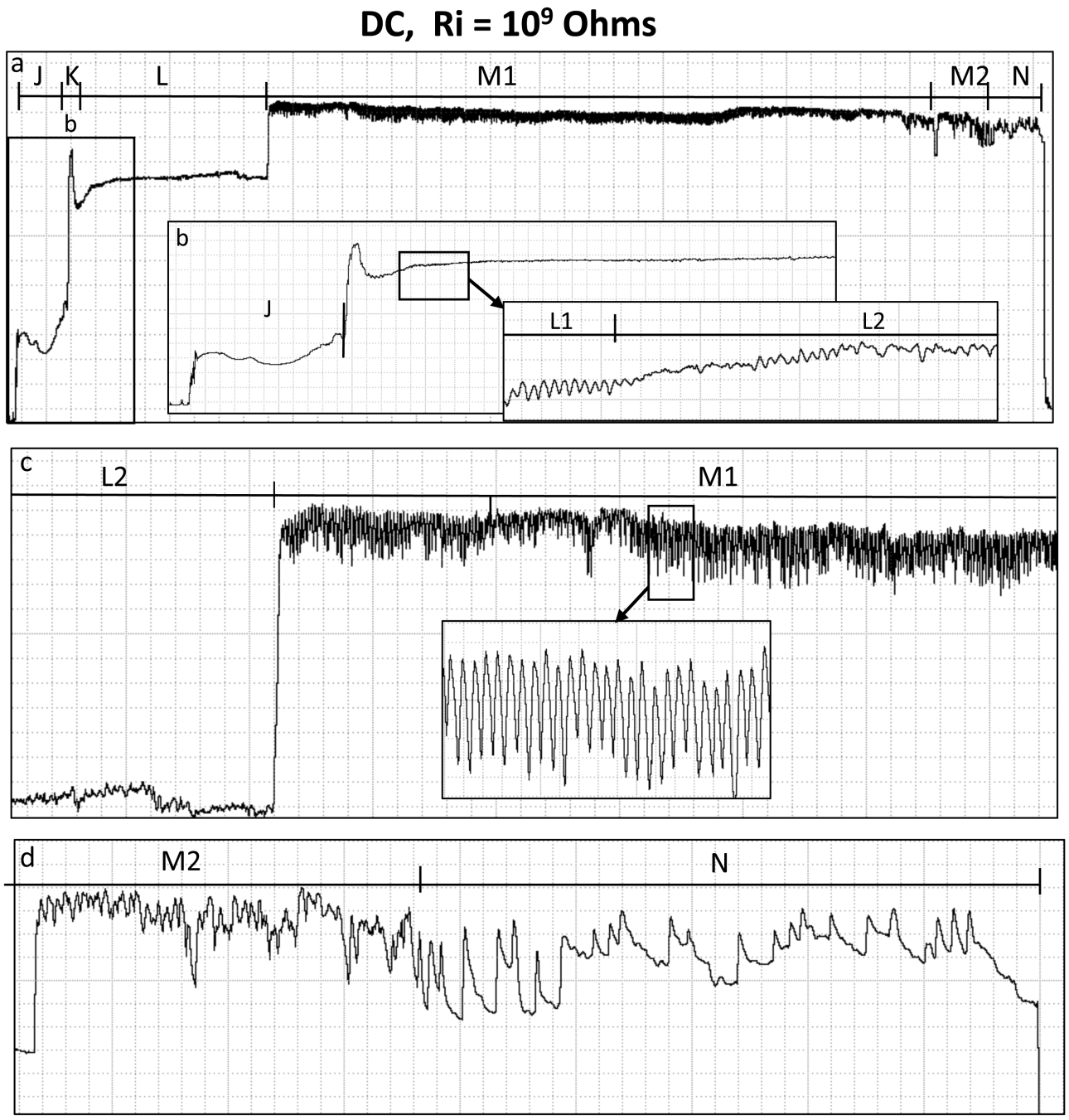

Fig. 5. Representative waveforms for EPG recordings at Ri = 10^9 Ohms, using applied signal 75 mV DC. (a) Overview of the entire mosquito stylet probe ('bite'). Family- and type-level names are along the top of the label bar. (b–d) Enlargements of boxes b–d in part (a). Labels similar to part (a). Time scales and Windaq gains were as follows: (a) 4 s/div, 8×; (b) 0.8 s/div, 8×, inset: 0.2 s/div, 64×; (c) 1 s/div, 32×, inset: 128×; (d) 0.4 s/div, 32×.

relatively unvarying throughout the entire event. A brief recording at Ri 10^{10} Ohms showed even smaller, flatter M (Fig. 7). Similar to L, there were no significant differences in numbers (NWEI), event durations (WDEI), or percentage of total probing represented by M (Table 2).

Like family L, family M was divided into two types, M1 and M2. M1 was a rhythmic and regular-frequency (5–16 Hz) wave, which occurred regardless of the voltage level (DC offset above the baseline) on which it rode. Fine structure differed according to the type of applied voltage. Using AC applied voltage, M1 was a modified sine wave at Ri 10^6–10^9 Ohms (Figs. 3c and 4a inset box; Fig. 5b, inset boxes; Fig. 8), each cycle being U-shaped, with pointed peaks oriented upwards or downwards in between round valleys and highly variable, peak-to-peak amplitude (Figs. 6a and 8). Occasionally, at 10^6 Ohms, an additional upward-going spike was seen at the end of each plateau of the sine wave (Fig. 2c). At very high Ri levels (10^{10} Ohms, Fig. 5b), M1 fine structure changed to a clear sine wave that did not change (except for smaller amplitude) (Figs. 6 and 8). Thus, M1 was highly recognizable with more details at all of the first four Ri levels. Using DC applied voltage, the variable-amplitude and detailed M1 signal was visible only at lower Ri levels of 10^6 and 10^7 Ohms (Fig. 8). At 10^8 and 10^9 Ohms, only the uniform, small-amplitude sine wave was visible, and at 10^{10} Ohms, the wave structure was almost completely flattened (Fig. 8).

Table 2. Descriptive statistics (mean, SEM) for three EPG variables for each mosquito waveform family described herein

	Variable	*P*-value	Ri = 10^6		Ri =10^7		Ri = 10^8		Ri = 10^9	
J	NWEI	<0.0001	(2) 0.17 ± 0.094	B	(9) 0.75 ± 0.094	A	(7) 1.00 ± 0.123	A	(10) 1.00 ± 0.103	A
	WDEI	0.0419	6.50 ± 1.403	A	2.74 ± 0.661	B	4.97 ± 0.750	A	4.85 ± 0.627	A
	%Prb – J	0.0030	0.39 ± 0.678	C	1.09 ± 0.678	BC	2.98 ± 0.888	AB	4.11 ± 0.743	A
K	NWEI	1.0000	(12) 1.00 ± 0.000		(12) 1.00 ± 0.000		(7) 1.00 ± 0.000		(10) 1.00 ± 0.000	
	WDEI	0.0299	5.77 ± 0.755	A	4.20 ± 0.755	AB	2.59 ± 0.989	B	2.72 ± 0.827	B
	%Prb – K	0.1206	3.08 ± 0.471		2.24 ± 0.471		1.40 ± 0.617		1.6703 ± 0.516	
L	NWEI	0.7328	(12) 1.92 ± 0.221		(12) 1.67 ± 0.221		(7) 2.00 ± 0.289		(10) 1.70 ± 0.242	
	WDEI	0.2792	28.82 ± 13.097		60.67 ± 13.097		26.29 ± 17.148		34.4333 ± 14.347	
	%Prb – L	0.5946	25.70 ± 4.666		34.48 ± 4.666		29.92 ± 6.109		32.3026 ± 5.111	
	TmFrm1stPrb – L	0.8074	6.85 ± 1.024		6.26 ± 1.024		7.56 ± 1.3407		7.57 ± 1.122	
M	NWEI	0.6901	(12) 1.58 ± 0.176		(12) 1.33 ± 0.176		(7) 1.43 ± 0.230		(10) 1.60 ± 0.192	
	WDEI	0.6361	105.73 ± 17.755		109.79 ± 17.755		85.20 ± 23.247		80.70 ± 19.450	
	%Prb – L	0.6740	66.50 ± 5.092		58.68 ± 5.092		62.8945 ± 6.668		58.7854 ± 5.578	
	TmFrm1stPrb – M	0.3667	38.53 ± 7.527		55.51 ± 7.527		37.6286 ± 9.855		43.77 ± 8.250	
N	NWEI	0.4914	(4) 0.33 ± 0.161		(6) 0.50 ± 0.161		(4) 0.57 ± 0.211		(6) 0.7 ± 0.176	
	WDEI	0.5345	18.60 ± 5.647		11.83 ± 4.610		8.75 ± 5.647		8.4167 ± 4.610	
	%Prb – L	0.9683	4.33 ± 2.063		3.51 ± 2.063		2.81 ± 2.702		3.1327 ± 2.260	
	TmFrm1stPrb – N	0.8580	153.05 ± 33.098		177.92 ± 27.025		176.63 ± 33.0981		150.75 ± 27.025	

Results of ANOVA comparing variables across Ri level (i.e., within rows) are summarized by capital letters; different letters in each row denote values that are significantly different at $\alpha = 0.05$. Numbers in parentheses on the first row of each waveform denote sample size of insects that performed that behavior in the comparison of 38 insects total. NWEI, (mean) number of waveform events per insect; WDEI (mean) waveform duration (in seconds) per event per insect; %Prb – waveform, percentage of the probe represented by that waveform, per insect; TmFrm1stPrb-L, time from the start of the probe to the first L; TmFrm1stPrb-M and TmFrm1stPrb-N, the equivalent for waveforms M and N.

These findings support that the unvarying, low-amplitude sine-wave M1 (best seen using DC at 10^8 Ohms or higher) was the emf component of the signal, while the variable amplitudes and modified peaks of the sine wave, as well as hooks/spikes on each plateau were R components of M1. The difference between AC and DC applied signals reflects the greater emphasis placed on pure R component with AC versus pure emf component with DC (see Discussion).

M2, similar to L2, was highly irregular with variable-frequency and variable-amplitude peaks and spikes, although usually taller than M1. M2 always followed the first M1 event. M2 duration was highly variable (Table 1), but often occurred in the second half of the probe (Ri 10^7–10^9 Ohms; Figs. 2a and c; 3a and c; 4a; and 5a and b). At all Ri levels, M1 was the dominant, near-exclusive waveform in the first half of ingestion phase.

Both M1 and M2 were visually correlated with abdominal swelling of the mosquito due to uptake of blood from the human host. Maxillary palpus oscillations also ceased during waveform M. Blood was observed in dissected mosquitoes when the insect initiated M ($N = 8$), even when the M duration was very short (2–3 s). Full engorgement, which occurred in 100% of the mosquito probes used in this dataset, was always correlated with family M.

Unknown Meaning, Family N

In the last seconds of half of the probes (48%) at all Ri levels, waveform family N often occurred. N resembled M2 in some respects such as voltage level, the same or larger amplitude, and irregular frequency and amplitude of individual peaks. However, N was distinctly different from all other waveform families and types in having consistently (much) lower frequency of its irregular spikes and peaks (Fig. 5c). N sometimes was difficult to distinguish from L but was determined to have a higher voltage level compared with baseline than did L. N was almost always performed after engorgement was complete and signaled the end of the probe just before stylet withdrawal. Family N was an almost-equal mixture of R and emf because its appearance was remarkably stereotypical at all Ri levels (data not shown), although amplitude and voltage level changed similar to L and M (data not shown). It could not be determined whether N was correlated with ingestion/engorgement, because most insects seemed replete by the time N began. Nonetheless, tiny amounts of salivation and/or ingestion might be occurring.

Transitional Probabilities of Mosquito Waveform Sequence

As shown in the *Ae. aegypti* kinetogram for typical probes (Fig. 9), the order of mosquito stylet activities represented by the waveforms was very stereotypical, especially until the beginning of M. A typical *Ae. aegypti* probe had the following waveform sequence: NP → J → K → L → M → N → Z where both NP and Z were added after recording to mark the beginning and end of the probe (Fig. 9). Sometimes, the insect alternated sequentially between L and M family waveforms. Sometimes a probe abruptly ended with M1 but, in other probes, stylet activities would return to L, sometimes activities would terminate in N. The kinetogram also clearly portrays the effect of Ri level on detection of J family waveforms. The transition from non-probing before the probe (NP, Fig. 9) was artifactually depressed to only 16.7% of the time at 10^6 Ohms, but 75% of the time at 10^7 Ohms. This disappearance of J was strictly due to the lack of detection of emf at lower Ri levels, because overt body postures and other signs of the pre-probing J behavior were performed by the mosquito at all Ri levels. There was no suppression of J at 10^8 or 10^9 Ohms. In contrast, the variation in transitional probabilities for L → M → N → Z (non-probing after the probe; Fig. 9) was caused by true variation in stylet activities by the mosquitoes, because all post-J waveforms were present and recognizable. There was only an 18% probability that probes ended directly after family M; the rest would either return to L (52% probability) or proceeded to a short event of waveform family N (30% probability). Ultimately, there was a 48% probability that the probe would end with N.

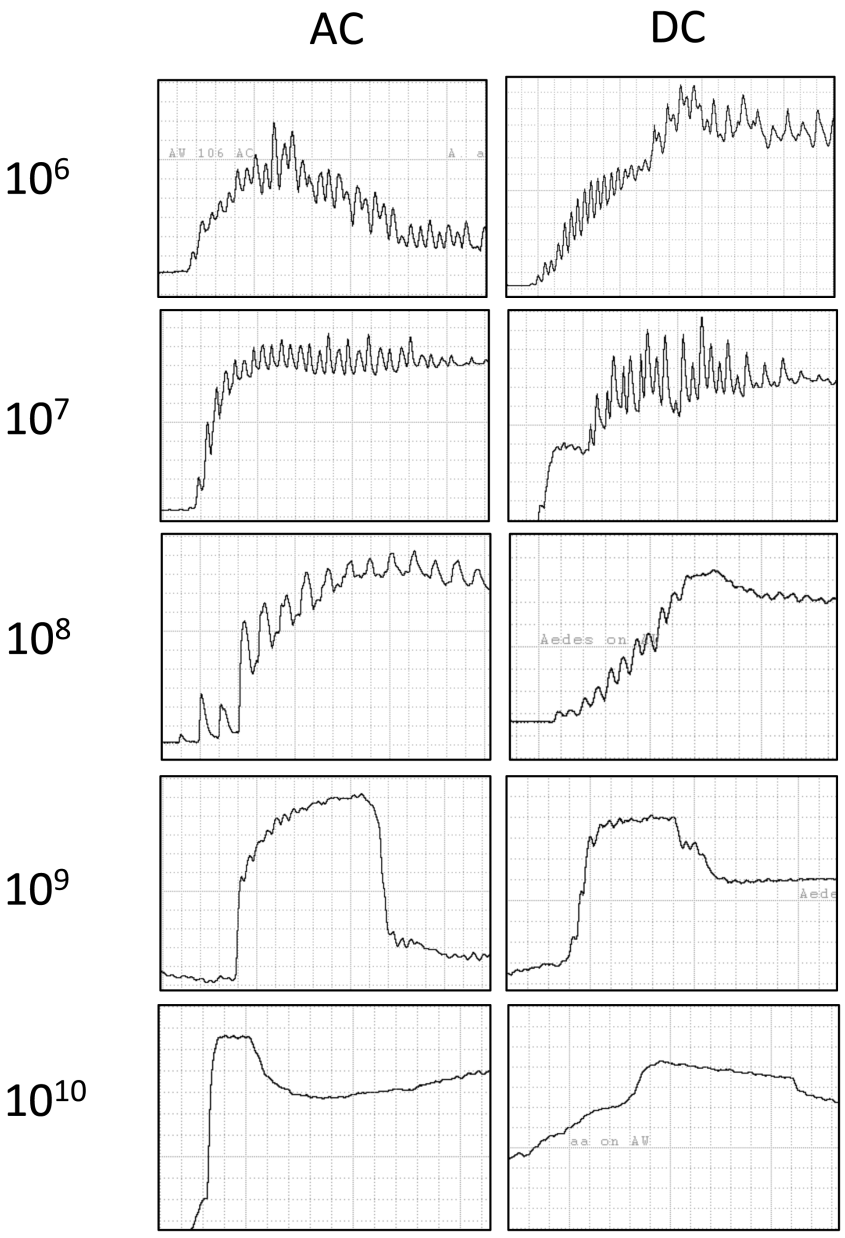

Fig. 6. Visual comparison of waveform K for AC versus DC applied voltages at Ri levels 10^6–10^{10} Ohms. Waveform appearance changes with Ri levels but not with applied signal type. Time scales for all views were at 0.2 s/div, Windaq gains for AC: (a) 10^6 64×, (b) 10^7 16×, (c) 10^8 32×, (d) 10^9 16×, (e) 10^{10} 8×. Windaq gains for DC: (f) 10^6 16×, (g) 10^7 16×, (h) 10^8 32×, (i) 10^9 32×, (j) 10^{10} 32×.

Discussion

Biological Meanings of Mosquito EPG Waveforms

We propose the following interpretations based on: 1) visual correlations (proboscis angle and depth, palpi movements, blood engorgement) with waveforms, 2) host sensory input (pain and other sensations), and 3) ingestion correlation with results from mosquito dissections. In addition, electrical origins were deduced from the appearances of the waveforms at differing Ri levels. While somewhat hypothetical, these interpretations match much of what is known or inferred from previous studies of mosquito stylet activities.

Pre-probing Phase, Family J

Waveform J represents initial proboscis contact with the skin and secretion of likely liquid, non-hardening saliva on the skin surface. This interpretation is supported because the initial, small waveform peak was the only R component in the waveform. Therefore, it was probably caused when liquid-coated stylet tips first contacted the skin. Dry stylet tips would not be very conductive. The subsequent short rise in voltage level (emf) at higher Ri levels shows maintenance of electrical contact. We hypothesize that analgesic, anti-coagulant saliva secreted on the skin surface could mask insertion of the stylets into the human host (Stark and James 1995, 1996; Ha et al. 2014).

Pathway Phase, Family K

Waveform K represents insertion and shallow penetration of at least the tips of the stylets into the skin, concomitant with near-continuous salivation. R-dominated peaks during K support that saliva that is more electrically conductive (thus probably more proteinaceous) than the saliva released during J was expelled in rapid spurts

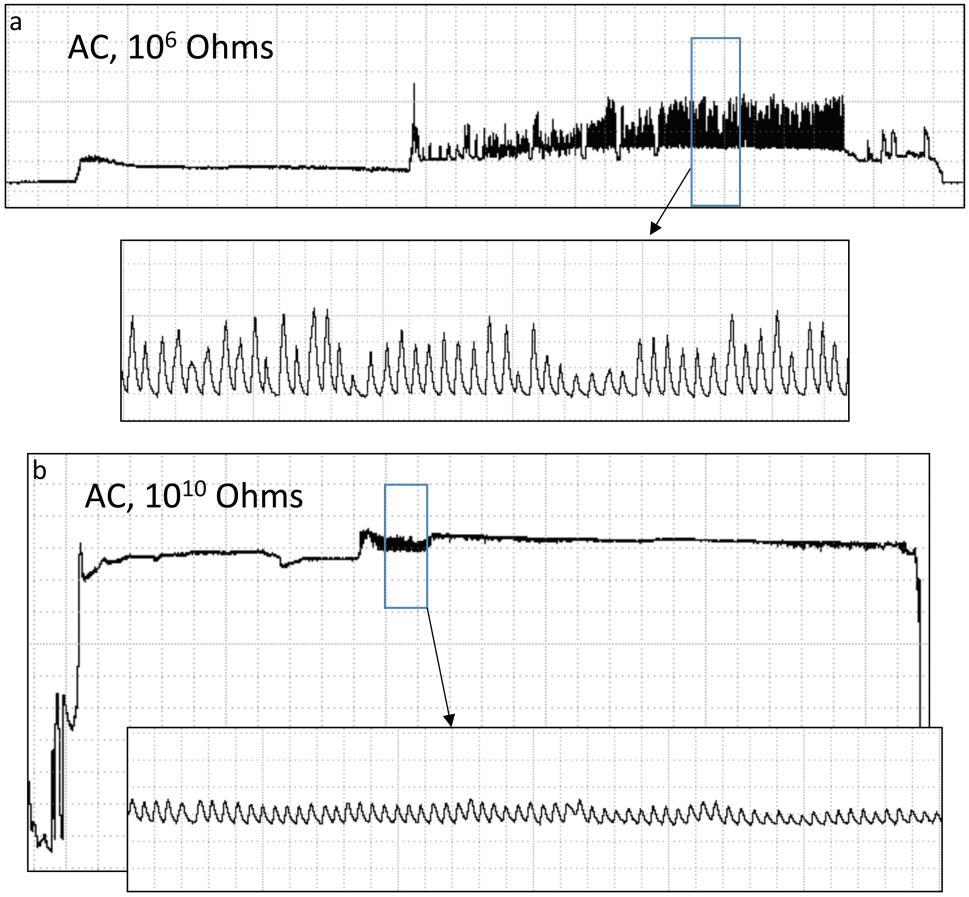

Fig. 7. Example M1 waveforms from 10^6 and 10^{10} Ohms, AC applied signal, highlighting the change in M1 sine wave amplitude as Ri level is increased. Parts (a) and (b) both have time scales of 4 s/div, Windaq gain 16×, with inset boxes: 0.2 s/div, 32×.

corresponding with the peaks. This would be consistent with observations of mosquito salivation during the early stages of mosquito probing (Griffiths and Gordon 1952, Gurera et al. 2018)—such saliva contains analgesic, anti-coagulant, and/or tissue-loosening proteins (Stark and James 1995, 1996; Ha et al. 2014). It is also possible that maxillary stylet fluttering (protraction–retraction) and/or side-to-side movements (R component) occurred during waveform K, providing a sawing action that could mechanically cut through the tough outer layers of skin.

Family L

Waveform L represented the bulk of pathway phase, when the stylets were penetrating deep skin tissues and searching for an acceptable blood vessel. Like K, waveform L was heavily R-dominated, thus likely representing salivary conductance and stylet movements. Visual observation of proboscis bending confirmed that, like pathway waveforms of sharpshooter leafhoppers and certain other hemipterans (Backus et al. 2005, Backus 2016), declining voltage levels at low Ri levels (thus, an R component) represent increasing depths as the stylets are pushed deeper into host tissue. Thus, L is the primary searching phase of stylet probing, i.e., seeking and finding a blood vessel from which to ingest, an activity first suggested by Ribeiro et al. (1984). Those authors hypothesized that salivation occurred in *Ae. aegypti* as the stylets moved towards a blood vessel and that this salivation was necessary for hematoma formation that facilitated blood vessel location. This is also consistent with Kebaier et al. (2009), who demonstrated deposition of *Plasmodium* sporozoites (via salivation) in/near dermal cells outside of blood vessels by *Anopheles stephensi*. Regular rhythmicity of L1 probably represents rhythmic stylet tip fluttering similar to that during K, but possibly wider and stronger ('drilling') with some salivation (Backus et al. 2005).

In the video of *Anopheles gambiae* (sensu lato) probing mouse ear tissue (Choumet et al. 2012), individual stylet tips were observed fluttering while traveling down through tissue to capillaries. The stylet tips could be seen to oscillate while approaching the capillary, then quickly inserting into the capillary within fractions of a second after making contact with the capillary wall. Although our recordings are of another species, we believe that the activity represented by the L waveform of *Ae. aegypti* is that same activity depicted in the *A. gambiae* mouse ear probing: movement towards a blood vessel.

Ingestion Phase: Family M

During engorgement, major uptake and swallowing of blood (ingestion) is represented by waveform family M. Blood is a highly proteinaceous liquid, with both cellular and non-cellular fractions; therefore, it is highly electrically conductive (Schwann 1983), unlike dilute phloem and xylem sap of plants. Thus, we propose that electrical conductivity accounts for the strong R domination of family M, especially the amplitude of M1 waves. This is in contrast to ingestion waveforms of aphids, which are strongly emf-dominated because less electrically conductive plant sap forms strong streaming potentials. The video of *A. gambiae* probing mouse ear tissue by Choumet et al. (2012) shows mosquito stylet tips rapidly inserting

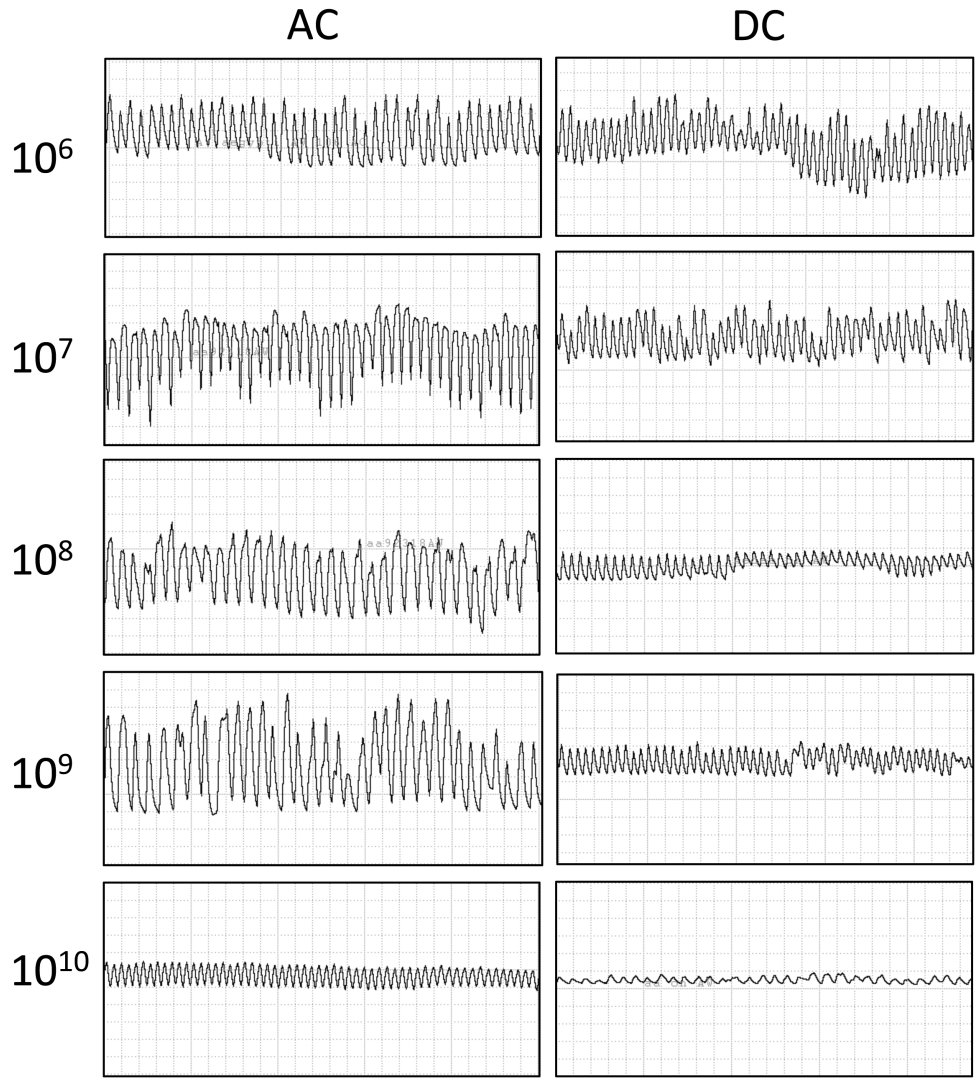

Fig. 8. Visual comparison of waveform M1 for AC versus DC applied voltages at Ri levels 10^6–10^{10} Ohms. Waveform appearance changes with both Ri levels and applied signal type. Time scales for all views were at 0.2 s/div, Windaq gains for AC: (a) 10^6 32×, (b) 10^7 16×, (c) 10^8 16×, (d) 10^9 16×, (e) 10^{10} 32×. Windaq gains for DC: (f) 10^6 16×, (g) 10^7 32×, (h) 10^8 32×, (i) 10^9 32×, (j) 10^{10} 32×.

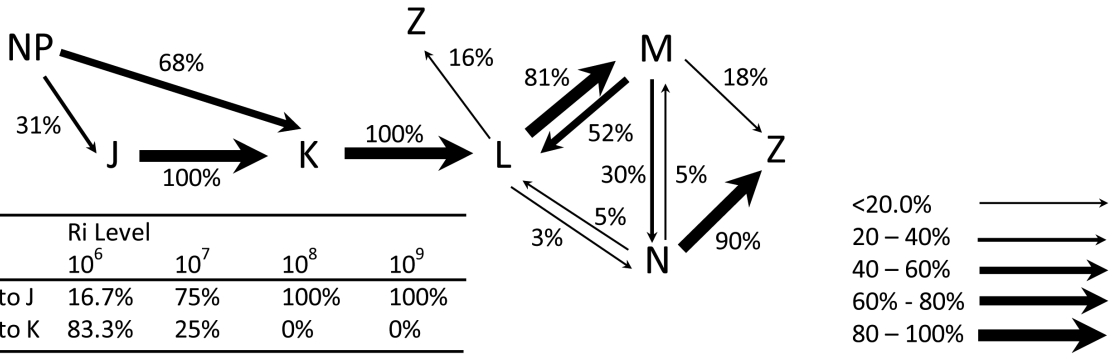

	Ri Level 10^6	10^7	10^8	10^9
NP to J	16.7%	75%	100%	100%
NP to K	83.3%	25%	0%	0%

Fig. 9. Kinetogram showing the probabilities that performance of certain waveforms transitioned into other waveform(s). Arrow width denotes certain levels of probability, as shown in the key on the right. Transitions from NP to either J or K are averaged across Ri levels for the chart, but actual percentages for each Ri level are shown in the table at lower left. NP, non-probing before the probe; Z, non-probing after the probe.

into a capillary tube. We propose that the immediate jump in voltage level observed in *Ae. aegypti* transitioning from L2 to M1 corresponds to the visually clear, rapid insertion of the stylets into a blood vessel. Of course, this interpretation and others could be best confirmed by combining video and EPG observation of mosquito feeding.

Interestingly, blood ingestion in mosquitoes is accomplished by two pumps, the cibarial and pharyngeal pumps (Pappas 1988), unlike in hemipterans, which have only a single, cibarial pump (Ammar 1985). We anticipated that blood pumping frequencies would vary greatly during mosquito ingestion, if each pump had its own pumping frequency that would sometimes interact, sometimes interfere with one another. However, this was not the case. Within a single insect, pumping frequency was relatively invariant, although a range of insect-specific frequencies was seen across multiple insects. In contrast to pumping frequency, amplitude of individual peaks in the M1 waveform varied strongly across the duration of an M1 event, usually the tallest peaks occurring during the first half of the ingestion event. We hypothesized that peak amplitude could be related to the degree of expansion of the cibarial or pharyngeal pumps, or both working in near-synchrony.

The dynamics of mosquito ingestion/pumping of in vitro sucrose solutions has been studied using electromyography and x-ray imaging. These studies show that, indeed, the pumps are sequentially coordinated; the cibarial and pharyngeal pumps fire nearly at the same time, but with a small phase lag (Kim et al. 2011, 2012, 2013). The most recent work (Kikuchi et al. 2018) demonstrated that there are two types of pumping: continuous pumping, in which the cibarial pump performs most of the work, and burst-mode pumping, in which the pharyngeal pump does most of the work. Furthermore, in continuous feeding, the cibarial pump does not expand to its greatest possible extent, and is acting as a pass-through to the pharyngeal pump (Kim et al. 2013, Kikuchi et al. 2018). In burst-mode feeding, both pumps are expanded to their fullest extent. In burst-mode feeding, both pumps are expanded to their fullest extent, providing 1.6× (cibarial) and 19× (pharyngeal) the maximum volume of continuous pumping (Kikuchi et al. 2018).

In studies of cibarial pumping in sharpshooter leafhoppers (Dugravot et al. 2008), sine wave (ingestion peak) amplitude was strongly correlated with the height of the cibarial diaphragm (the lid of the pump); the higher the amplitude, the higher the uplift of the pump lid, thus the greater the expansion of the pump. Uplift was a strong R component (Dugravot et al. 2008). Similarly, we believe that degree of pump expansion in mosquitoes feeding is indicated by amplitude of the M1 peak.

Kikuchi et al. (2018) proposed two hypotheses to explain the behavioral role of maximal pharyngeal pump expansion (thus a very large vacuum at the tip of the proboscis) in burst-mode feeding: 1) the 'clearance' hypothesis, to clear blockages in the system, and 2) the 'priming' hypothesis, to prime the food canal at the start of pumping. We agree with the likelihood of both of these hypotheses. However, our work strongly suggests a third, which we term the 'big gulp' hypothesis. The idea was actually suggested by Kikuchi et al. (2018), who explain that burst-mode feeding could 'provide quick boosts in volume flow rate, enabling faster drinking bouts that would help the mosquito to avoid detection'. They also state that blood, unlike sugar water, is a non-Newtonian liquid, whose properties may influence the way pumping of blood could differ from that of sugar water. Also, Kikuchi et al. (2018) point out that capillary blood pressure is positive, and might aid in pumping, as it does in aphids (Tjallingii 1995). Accordingly, ingestion of blood may utilize burst-mode feeding much more than does ingestion of sugar water, supporting its use in the beginning of virtually every blood-ingestion event, as seen in our work. We therefore propose that the high-amplitude M1 peaks at the beginning of virtually every blood-ingestion (M1) event ('drinking bout' of Kikuchi et al. [2018]) represent burst-mode feeding. Thus, our work supports the idea that maximal pumping is required early in each stylet probe, due to the mosquito's need to quickly engorge and then depart the host.

Finally, one more M1 appearance deserves mention. Often at Ri 10^6 Ohms (Fig. 2), but not always (Fig. 8), the wave in M1 was less like a sine wave and more like a series of flat-topped plateaus with a prominent spike at the end of every plateau. A similar appearance has been attributed to muscular closure of the precibarial valve below the cibarium in sharpshooters and other leafhoppers (Backus et al. 2005, Backus 2016). Although there is a pharyngeal valve between the cibarial and pharyngeal pumps in mosquitoes, it is not thought to act as a pressure-sensitive check valve (Kim et al. 2013). Therefore, we are unsure of the meaning of this spike in mosquito ingestion.

We hypothesize that most of the R-dominated details in the M1 waveform derive from pumping highly electrically conductive blood, whose R component would mask the much smaller emf component. At Ri 10^9 Ohms, streaming potentials of blood pumping during M1 are revealed as lower-amplitude, near-perfect sine waves. It is also possible that tiny amounts of saliva are also simultaneously secreted during M1 ingestion, which is consistent with observations of Griffiths and Gordon (1952), similar to aphid ingestion/salivation during E2 (Tjallingii 1995). However, the R component of M1 salivation is probably masked by high conductivity of blood relative to saliva.

M2, like L2, may represent cessation (or at least reduction) of rhythmic pumping and replacement with copious salivation into a blood vessel. In hemipteran EPG, variable-frequency but continuous waves similar to L2 and M2 usually indicate salivation, perhaps mixed with ingestion. We hypothesize that, after continuous pumping/ingestion by mosquitoes has occurred for a while, blood coagulation begins to plug the vessel, similar to what happens in phloem sieve elements during aphid ingestion. In the case of aphids, watery saliva is then secreted to break up the plug (Medina-Ortega and Walker 2013). Therefore, we further hypothesize that mosquitoes secrete saliva, known to contain the anti-coagulant heparin (Ha et al. 2014) under similar circumstances and that L2 and M2 may represent such salivation. Once the blood vessel is wholly-to-partially re-opened, the mosquito can begin pumping again, hence the alternation of M1 and M2 events towards the end of the probe. Although no direct evidence for this idea exists at present, EPG could be used to test this hypothesis.

Ingestion Phase: Family N

Family N is a mixture of R and emf, with low frequency, irregular spikes and peaks. This suggests a mixture of stylet movement, salivation, and streaming potentials. However, it is unknown whether blood is being taken up during N, or whether the insect is no longer ingesting but in the process of removing its stylets from the blood vessel and then skin, perhaps with some salivation (as occurs at the termination of most leafhopper probes [Backus et al. 2005]).

Optimum Ri Settings for Future *Ae. aegypti* EPG Studies

Based on the present results, we recommend that future researchers choose either 10^7 or 10^8 Ohms to achieve the best balance of R to emf, depending on which waveforms/behaviors are of greatest interest. For K or L waveforms, choose 10^7 Ohms; for M waveforms, choose 10^8 Ohms. We do not recommend 10^6 Ohms for quantitative studies because waveform J (pre-probing) was not visible and waveform K (initial stylet penetration) had artificially lengthened

event durations. We also do not recommend 10^9 Ohms because most waveforms are distorted in appearance or difficult to identify. Either AC or DC is appropriate for EPG studies of mosquitoes in a noise-free environment.

Application of Modern EPG to Mosquito Biology

EPG has long been used to study hemipteran feeding behavior and has been an invaluable tool to describe basic stylet probing activities of aphids, leafhoppers, whiteflies, and other taxa as they interact with their host plants. This technology has enabled the study of host plant defense responses (Rangasamy et al. 2015), effect of insecticides upon feeding behavior (Wayadande and Backus 1989, Serikawa et al. 2012), acquisition and inoculation of phytopathogenic bacteria and viruses (Wayadande and Nault 1994, Jing et al. 2015), and descriptive biology of vector–plant–pathogen interactions (Wayadande and Nault 1996).

The early attempts to quantify precise mouthpart activities of mosquitoes were somewhat successful, but could be improved greatly by use of EPG. New EPG technology has been improved electronically to the point of feasibility for the quantitative and qualitative study of blood-sucking arthropods. In tandem with the improvements in EPG capabilities, digital microscopy and videography have advanced immensely. As a result, highly accurate descriptions of mosquito stylet movement in animal tissue have been previously accomplished (Ribeiro et al. 1984, Choumet et al. 2012). Nonetheless, no descriptive studies have provided detailed quantifiable information about precise stylet activities. Also, precise studies of mosquito blood flow through the food canal (Lee et al. 2009, Kikuchi and Mochizuki 2011) are extremely labor intensive and are not amenable to detection of biological variation within a large sample size of insects. Although the previous two studies provided precise quantification of flow rates, they also used free blood instead of host animals, which very likely influenced the results. Using EPG, researchers can work with living insects and hosts whose activities likely reflect more closely those performed in a natural environment. If EPG was combined with digital microscopy and videography techniques (Lee et al. 2009, Kikuchi and Mochizuki 2011), a truly ground-breaking study could be accomplished.

EPG studies of mosquitoes can answer many important questions. For example, do all mosquito species produce stereotypical sequences of probing culminating in blood ingestion? What level of variation exists between individuals of the same species, or species in the same genus? Is there variation among individuals that feed on different types of hosts? We know that hemipterans display this type of variation (feeding plasticity), and it is extremely important in discerning host plant resistance genes or effect of pesticides. We have demonstrated here that even though *Ae. aegypti* probes are very similar in behaviors performed, there is still considerable variation among individuals with respect to entire probe duration, duration of penetration to a capillary vessel, and duration of various waveforms. Our kinetogram also demonstrated that *Ae. aegypti* recorded (even under our highly standardized conditions) displays behavioral plasticity, i.e., variation of performance of behaviors on different hosts, for some of the behaviors.

Better understanding of mosquito feeding could lead to exciting applications, such as possible use of mosquitoes to deliver vaccines to mammalian hosts (Spring et al. 2013) or to deliver dsRNA for RNAi applications (Mutti et al. 2008). EPG could be used to precisely quantify average delivery time and accuracy for particular vector species, once the baseline information was collected and analyzed describing inoculation behavior. Another application might be in host resistance (induced by repellents or genetically) to mosquito bites and/or subsequent inoculation of pathogens like Zika virus or *Plasmodium*. Thus, we believe that use of EPG for mosquito biology might open important doorways into the types of fruitful and insightful research that has been pursued for decades with hemipteran pathogen vectors and pests.

Acknowledgments

Support for A.C.W. and B.H.N. was provided by the Oklahoma Agricultural Experiment Station (OKL03168 and OKL03085). Funding for E.A.B. was provided by United States Department of Agriculture-Agricultural Research Service appropriated project #2034-22000-010-00D. We thank Victoria Pickens for operating equipment during EPG sessions. We also thank Dr. James Throne, ARS Parlier, and two anonymous reviewers for their helpful suggestions on an earlier draft of this manuscript.

References Cited

Ammar, E. D. 1985. Internal anatomy of leafhoppers and planthoppers, pp. 127–162. *In* L. R. Nault and J. G. Rodriguez (eds.), The leafhoppers and planthoppers. Plenum Press, New York.

Backus, E. A. 2016. Sharpshooter feeding behavior in relation to transmission of *Xylella fastidiosa*: a model for foregut-borne transmission mechanisms, pp. 175–194. *In* J. K. Brown (ed.), Vector-mediated transmission of plant pathogens. American Phytopathological Society Press, St. Paul, MN.

Backus, E. A., and W. H. Bennett. 2009. The AC-DC correlation monitor: new EPG design with flexible input resistors to detect both R and emf components for any piercing-sucking hemipteran. J. Insect Physiol. 55: 869–884.

Backus, E. A., M. J. Devaney, and W. H. Bennett. 2000. Comparison of signal processing circuits among seven AC electronic monitoring systems for their effects on the emf and R components of aphid (Homoptera: Aphididae) waveforms, pp. 102–143. *In* G. P. Walker and E. A. Backus (eds.), Principles and applications of electronic monitoring and other techniques in the study of homopteran feeding behavior. Entomological Society of America, Lanham, MD.

Backus, E. A., J. Habibi, F. M. Yan, and M. R. Ellersieck. 2005. Stylet penetration by adult glassy-winged sharpshooter on grape: EPG waveform characterization, tissue correlation and possible implications for transmission of *Xylella fastidiosa*. Ann. Entomol. Soc. Am. 98: 787–813.

Backus, E. A., F. A. Cervantes, R. Narciso Guedes, A. Y. Li, and A. C. Wayadande. 2019. AC-DC electropenetrography (EPG) for in-depth studies of oviposition and piercing-sucking feeding behaviors. Special Collection of Ann. Entomol. Soc. Am. 112: 236–248. doi:10.1093/aesa/saz009

Brickley, E. B., M. Coulibaly, E. E. Gabriel, S. A. Healy, J. C. C. Hume, I. Sagara, S. F. Traore, O. Doumbo, and P. E. Duffy. 2016. Utilizing direct skin feeding assays for development of vaccines that interrupt malaria transmission: a systematic review of methods and case study. Vaccine 34: 5863–5870.

Cervantes, F. A., and E. A. Backus. 2018. EPG waveform library for *Graphocephala atropunctata* (Hemiptera: Cicadellidae): effect of adhesive, input resistor, and voltage levels on waveform appearance and stylet probing behaviors. J. Insect Physiol. 109: 21–40.

Choumet, V., T. Attout, L. Chartier, H. Khun, J. Sautereau, A. Robbe-Vincent, P. Brey, M. Huerre, and O. Bain. 2012. Visualizing non infectious and infectious *Anopheles gambiae* blood feedings in naive and saliva-immunized mice. PLoS ONE 7: e50464.

Dugravot, S., E. A. Backus, B. J. Reardon, and T. A. Miller. 2008. Correlations of cibarial muscle activities of *Homalodisca* spp. sharpshooters (Hemiptera: Cicadellidae) with EPG ingestion waveform and excretion. J. Insect Physiol. 54: 1467–1478.

Ebert, T. A., E. A. Backus, M. Cid, A. Fereres, and M. Rogers. 2015. A new SAS program for behavioral analysis of electrical penetration graph data. Comput. Electron. Agric. 116: 80–87.

Fereres, A., and Collar, J. L. 2001. Analysis of noncirculative transmission by electrical penetration graphs, pp. 87–109. *In* K. F. Harris, O. P. Smith, and

J. E. Duffus (eds.), Virus-insect-plant interactions. Academic Press, New York.

Griffiths, R. B., and R. M. Gordon. 1952. An apparatus which enables the process of feeding by mosquitoes to be observed in the tissues of a live rodent; together with an account of the ejection of saliva and its significance in Malaria. Ann. Trop. Med. Parasitol. 46: 311–319.

Gurera, D., B. Bhushan, and N. Kumar. 2018. Lessons from mosquitoes' painless piercing. J. Mech. Behav. Biomed. Mater. 84: 178–187.

Ha, Y. R., S. R. Oh, E. S. Seo, B. H. Kim, D. K. Lee, and S. J. Lee. 2014. Detection of heparin in the salivary gland and midgut of *Aedes togoi*. Korean J. Parasitol. 52: 183–188.

Jing, P., L. Huang, S. Bai, and F. Liu. 2015. Effects of rice resistance on the feeding behavior and subsequent virus transmission efficiency of *Laodelphax striatellus*. Arthropod-Plant Interactions 9: 97–105.

Joost, P. H., E. A. Backus, D. Morgan, and F. Yan. 2006. Correlation of stylet activities by the glassy-winged sharpshooter, *Homalodisca coagulata* (Say), with electrical penetration graph (EPG) waveforms. J. Insect Physiol. 52: 327–337.

Kashin, P. 1966. Electronic recording of the mosquito bite. J. Insect Physiol. 12: 281–284.

Kashin, P., and B. E. Arneson. 1969. An automated repellency assay system. II. A new electronic "Bitometer-timer". J. Econ. Entomol. 62: 200–205.

Kashin, P., and H. G. Wakeley. 1965. An insect "bitometer'. Nature 208: 462–446.

Kebaier, C., T. Voza, and J. Vanderberg. 2009. Kinetics of mosquito-injected *Plasmodium* sporozoites in mice: fewer sporozoites are injected into sporozoite-immunized mice. PLoS Pathog. 5: e1000399.

Kikuchi, K., and O. Mochizuki. 2011. Micro-PIV (micro particle image velocimetry) visualization of red blood cells (RBCs) sucked by a female mosquito. Measurement Sci. Tech. 22: 064002.

Kikuchi, K., M. A. Stremler, S. Chatterjee, W. K. Lee, O. Mochizuki, and J. J. Socha. 2018. Burst mode pumping: a new mechanism of drinking in mosquitoes. Sci. Rep. 8: 4885.

Kim, B. H., H. K. Kim, and S. J. Lee. 2011. Experimental analysis of the blood-sucking mechanism of female mosquitoes. J. Exp. Biol. 214: 1163–1169.

Kim, B. H., E. S. Seo, J. H. Lim, and S. J. Lee. 2012. Synchrotron X-ray microscopic computed tomography of the pump system of a female mosquito. Microsc. Res. Tech. 75: 1051–1058.

Kim, B. H., H. Ha, E. S. Seo, and S. J. Lee. 2013. Effect of fluid viscosity on the liquid-feeding flow phenomena of a female mosquito. J. Exp. Biol. 216: 952–959.

Lee, S. J., B. H. Kim, and J. Y. Lee. 2009. Experimental study on the fluid mechanics of blood sucking in the proboscis of a female mosquito. J. Biomech. 42: 857–864.

Lutz, E. K., C. Lahondère, C. Vinauger, and J. A. Riffell. 2017. Olfactory learning and chemical ecology of olfaction in disease vector mosquitoes: a life history perspective. Curr. Opin. Insect Sci. 20: 75–83.

Maekawa, E., H. Aonuma, B. Nelson, A. Yoshimura, F. Tokunaga, S. Fukumoto, and H. Kanuka. 2011. The role of proboscis of the malaria vector mosquito *Anopheles stephensi* in host-seeking behavior. Parasit. Vectors 4: 10.

McLean, D. L., and M. G. Kinsey, 1964. A technique for electronically recording aphid feeding and salivation. Nature 202: 1358–1359.

McLean, D. L., and Kinsey, M. G. 1967. Probing behavior of the pea aphid, *Acyrthosiphon pisum*. I. Definitive correlation of electronically recorded waveforms with aphid probing activities. Ann. Entomol. Soc. Am. 60: 400–405.

Medina-Ortega, K. J., and Walker, G. P. 2013. Does aphid salivation affect phloem sieve element occlusion in vivo? J. Exper. Botany 64: 5525–5535.

Mutti, N. S., J. Louis, L. K. Pappan, K. Pappan, K. Begum, M. S. Chen, Y. Park, N. Dittmer, J. Marshall, J. C. Reese, et al. 2008. A protein from the salivary glands of the pea aphid, *Acyrthosiphon pisum*, is essential in feeding on a host plant. Proc. Natl Acad. Sci. USA 105: 9965–9969.

Pappas, L. G. 1988. Stimulation and sequence operation of cibarial and pharyngeal pumps during sugar feeding by mosquitoes Ann. Entomol. Soc. Am. 81: 274–277.

Rangasamy, M., H. J. McAuslane, E. A. Backus, and R. H. Cherry. 2015. Differential probing behavior of *Blissus insularis* (Hemiptera: Blissidae) on resistant and susceptible St. Augustinegrasses. J. Econ. Entomol. 108: 780–788.

Ray, A. 2015. Reception of odors and repellents in mosquitoes. Curr. Opin. Neurobiol. 34: 158–164.

Ribeiro, J. M., P. A. Rossignol, and A. Spielman. 1984. Role of mosquito saliva in blood vessel location. J. Exp. Biol. 108: 1–7.

Robinson, A., A. O. Busula, M. A. Voets, K. B. Beshir, J. C. Caulfield, S. J. Powers, N. O. Verhulst, P. Winskill, J. Muwanguzi, M. A. Birkett, et al. 2018. Plasmodium-associated changes in human odor attract mosquitoes. Proc. Natl Acad. Sci. USA 115: E4209–E4218.

Schwann, H. P. 1983. Electrical properties of blood and its constituents: alternating spectroscopy. Blut. 46: 185–197.

Serikawa, R. H., E. A. Backus, and M. E. Rogers. 2012. Effects of soil-applied imidacloprid on Asian citrus psyllid (Hemiptera: Psyllidae) feeding behavior. J. Econ. Entomol. 105: 1492–1502.

Spring, M., J. Murphy, R. Nielsen, M. Dowler, J. W. Bennett, S. Zarling, J. Williams, P. de la Vega, L. Ware, J. Komisar, et al. 2013. First-in-human evaluation of genetically attenuated *Plasmodium falciparum* sporozoites administered by bite of *Anopheles* mosquitoes to adult volunteers. Vaccine 31: 4975–4983.

Stark, K. R., and A. A. James. 1995. A factor Xa-directed anticoagulant from the salivary glands of the yellow fever mosquito *Aedes aegypti*. Exp. Parasitol. 81: 321–331.

Stark, K. R., and A. A. James. 1996. Salivary gland anticoagulants in culicine and anopheline mosquitoes (Diptera:Culicidae). J. Med. Entomol. 33: 645–650.

Tariq, K., M. Noor, E. A. Backus, A. Hussain, A. Ali, W. Peng, and H. Zhang. 2017. The toxicity of flonicamid to cotton leafhopper, *Amrasca biguttula* (Ishida), is by disruption of ingestion: an electropenetrography study. Pest Manag. Sci. 73: 1661–1669.

Tjallingii, W. F. 1978. Electronic recording of penetration behaviour by aphids. Entomol. Exp. Appl. 24: 721–730.

Tjallingii, W. F. 1985. Electrical nature of recorded signals during stylet penetration by aphids. Entomol. Exp. Appl. 38: 177–186.

Tjallingii, W. F. 1995. Regulation of the phloem sap feeding by aphids, pp. 190–209. *In* R. F. Chapman and G. de Boer (eds.), Regulatory mechanisms in insect feeding. Springer, Boston, MA.

Tjallingii, W. F., and T. Hogen Esch. 1993. Fine structure of aphid stylet routes in plant tissues in correlation with EPG signals. Physiol. Entomol. 18: 317–328.

Tjallingii, W. F. and E. Prado. 2001. Analysis of circulative transmission by electrical penetration graphs, pp. 87–109. *In* K. F. Harris, O. P. Smith, and J. E. Duffus (eds.), Virus-insect-plant interactions. Academic Press, New York.

Walker, G. P. 2000. A beginner's guide to electronic monitoring of homopteran probing behavior, pp. 14–40. *In* G. P. Walker and E. A. Backus (eds.), Principles and applications of electronic monitoring and other techniques in the study of homopteran feeding behavior. Entomological Society of America (Thomas Say Publications in Entomology).

Wayadande, A. C., and E. A. Backus. 1989. Probing behavior of the potato leafhopper (Homoptera: Cicadellidae) on chlordimeform- and phosmet-treated alfalfa. J. Econ. Entomol. 82: 766–772.

Wayadande, A., and L. R. Nault. 1994. Leafhopper probing behavior associated with maize chlorotic dwarf virus transmission to maize. Phytopathology 83:522–526.

Wayadande, A. C., and L. R. Nault. 1996. Leafhoppers on leaves: an analysis of feeding behavior using conditional probabilities. J. Insect Behavior 9: 3–21

World Health Organization (WHO). 2017. Vector-borne diseases. (https://www.who.int/news-room/fact-sheets/detail/vector-borne-diseases). Accessed June 2019.

Zhou, Y. H., Z. W. Zhang, Y. F. Fu, G. C. Zhang, and S. Yuan. 2018. Carbon dioxide, odorants, heat and visible cues affect wild mosquito landing in open spaces. Front. Behav. Neurosci. 12: 86.

Zwiebel, L. J., and W. Takken. 2004. Olfactory regulation of mosquito-host interactions. Insect Biochem. Mol. Biol. 34: 645–652.